# Magnetic normal modes of nano-elements

R. D. McMichael and M. D. Stiles

*National Institute of Standards & Technology,*

*Gaithersburg, Maryland 20899, USA*

(Dated: DRAFT: September 1, 2004)

## Abstract

Micromagnetic calculations are used to determine the eigenfrequencies and precession patterns of some of the lowest-frequency magnetic normal modes of submicron patterned elements. For a Permalloy-like ellipse, 350 nm × 160 nm × 5 nm thick in zero field, the lowest frequency normal mode at 4 GHz corresponds to precession in the "ends" of the ellipse. This mode is not predicted by quantization of wavevectors in the confined geometry. The eigenmodes of a normally magnetized 50 nm diameter × 15 nm thick cobalt disk are calculated. The calculated eigenfrequencies increase linearly with applied field, mimicking the behavior of the experimental critical current for spin transfer instabilities in an experimental realization of this disk.

## I. INTRODUCTION

Knowledge of the magnetic normal modes is valuable for understanding the thermal noise behavior of small magnetic elements such as those in sensors or MRAM cells. A number of experimental investigations of normal modes have been carried out on micron-scale patterned elements including squares in remnant states[1,2], on squares[3,4] and circles[3,5–7] in vortex states and on thin strips[8–10]. There are relatively few theoretical investigations of normal modes in magnetic patterned elements, mostly due the difficulty of dealing with nonuniform magnetostatic fields[11,12]. Grimsditch et al. have used micromagnetic techniques to examine the normal modes of a small rectangular block, comparing the computed frequencies to frequencies calculated from infinite film dispersion relations with discrete wavevectors[13].

While normal modes are can describe dynamics only for linear dynamics, they are also useful for understanding the instabilities that lead to nonlinear phenonomena such as switching and large amplitude oscillations driven by applied fields or spin transfer torques.

While spin transfer effects are most frequently observed in systems with two magnetic layers they have been been observed[14–16] and calculated[17,18] in systems with a single magnetic layer. In single films, a proper description of spin transfer instabilities requires a tight integration of a transport calculation with a micromagnetic calculation. Calculations done to date[17,18] have focused on the transport calculation at the cost of using an oversimplified treatment of the micromagnetic interactions. The most important simplification is that the samples are treated as infinite layers with magnetostatics either ignored or treated as a uniaxial anisotropy. To understand the consequences of this oversimplification, we have computed the normal modes of some of the measured samples[14]. In these samples, the ferromagnetic layer is more like a disk than a thin film so that the modes are very different from thin film modes.

This paper explores the normal modes of two nanometer-scale patterned bits, one a thin-film ellipsoid that illustrates the computational technique and the other is a short cylinder that models the magnetic nanoelement in a spin-transfer torque experiment[14].

The micromagnetic calculations were performed using the NIST micromagnetic test code, OOMMF[19]. Starting with a minimum energy state, the magnetization is excited by a short, strong field pulse so that magnetic moments were rotated a maximum of approximately 10°. In general this field pulse was not uniform. Field pulses with different symmetries were used

to excite normal modes with corresponding symmetries. After the field pulse, the evolution of the magnetization was calculated using the Landau-Lifshitz equations of motion with Gilbert damping and $\alpha = 0.01$. The evolution of the magnetization during the ringdown was captured by saving the magnetization configuration $\mathbf{M}(\mathbf{r}_i, t_j)$ at uniform time intervals. In many cases, the ringdown appears as a complicated wiggling of the magnetization when viewed as an animation. However, when viewed in the frequency domain, the apparently complicated behavior can be understood as the superposition of a few normal modes.

For each point $\mathbf{r}_i$ in the magnetic element, the ringdown record contains a time series of the magnetization at that point. Local power spectra of the magnetization are constructed by performing a discrete Fourier transform,

$$S_x(\mathbf{r}_i, f) = \left[ \sum_j M_x(\mathbf{r}_i, t_j) e^{i2\pi f\, t_j}. \right]^2 \tag{1}$$

To obtain an overall view of the magnetization behavior, the power spectra are summed over $\mathbf{r}_i$.

$$\bar{S}_x(f) = \sum_i S_x(\mathbf{r}_i, f). \tag{2}$$

Note that $\bar{S}$ is very different from the power spectrum of the spatially averaged magnetization. We find that plots of $\bar{S}(f)$ exhibit many peaks corresponding to oscillations at eigenfrequencies of the magnetization. At these peak frequencies, $S(\mathbf{r}_i, f)$ gives a map of the precession amplitude for the excited mode.

## II. THIN ELLIPSE

We have calculated linear magnetization dynamics for a 160 nm × 350 nm × 5 nm ellipse of Permalloy in zero applied field using 2.5 × 2.5 × 5 nm$^3$ cells. The relaxed state of this ellipse has nearly uniform magnetization aligned with the long axis of the ellipse in the central region but nearer to the edges, the magnetization tends to follow the edge contour, except at the ends where the magnetization points normal to the edge.

Field pulses with different spatial symmetries were used to highlight different normal modes. The modes are shown along the top of fig. 1. The modes excited by a uniform field pulse include the lowest frequency mode corresponding to motion near the "ends" of the ellipse where the magnetization has a large component normal to the edge. Also excited are

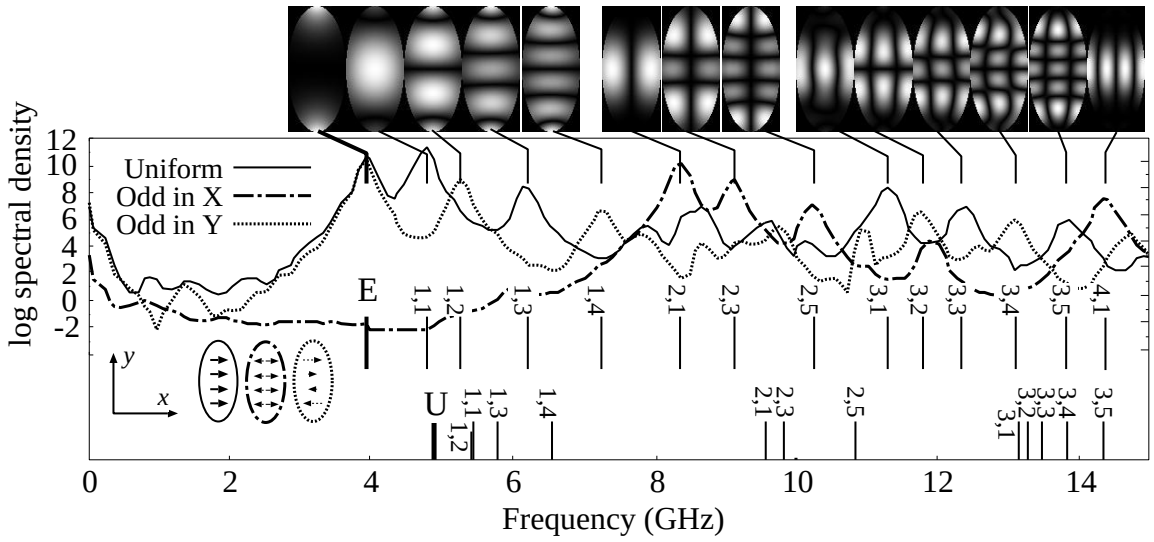


FIG. 1: Eigenmode images (top) and spatially averaged power spectra (middle) for a 160 nm × 350 nm × 5 nm ellipse of Permalloy in zero applied field. The spectra and images were obtained from three time series following excitation field pulses with three different symmetries. The mode frequencies are compared with frequencies calculated from a spinwave dispersion relation (bottom). The line labeled "U" is calculated for precession of uniform magnetization.

a mode with large amplitude in the center and a series of modes with even numbers of nodal lines running parallel and perpendicular to the symmetry axes of the sample. To excite other modes, we have used excitation pulses with other symmetries, including field pulses with field amplitudes proportional to $x$ or $y$ as measured from the center of the sample. The end modes have nearly the same resonant frequency whether the precession in the ends is in phase (uniform pulse) or out of phase (odd-$y$ pulse). This indicates that the ends of the ellipse interact very weakly.

We have attempted to explain the observed spectra using analytical models that include the effects of applied field, exchange and magnetostatic interactions. The magnetostatic interactions can be approximated two ways: 1) by calculating demagnetization factors for uniform magnetization or 2) by using the dispersion relation for spinwaves in infinite thin films and selecting discrete wavevectors appropriate for the sample geometry.

Because the sample is not an ellipsoid, the magnetostatic fields are not uniform. We calculate spatially averaged demagnetization factors for the ellipse using $E_d = \frac{1}{2} V_s \mu_0 N_\alpha M_\alpha^2$ for uniform $\mathbf{M}$ pointing in the $x$, $y$ and $z$ directions to yield $N_x = 0.0515$, $N_y = 0.0182$, and $N_z = 0.931$. For an ellipsoid with the same demagnetization factors, the precession frequency

for uniform magnetization is $\omega = \gamma\mu_0 M_s\sqrt{(N_x - N_y)(Nz - Ny)}$ or $f = 4.91$ GHz, marked as "U" in fig. 1. The gyromagnetic ratio, $\gamma = 2.11 \times 10^5$ m/As and $M_s = 8 \times 10^5$ A/m.

To estimate frequencies for nonuniform modes, we use the dispersion relation for an infinite thin film. At zero applied field with the magnetization in plane,

$$\left(\frac{\omega(\mathbf{k})}{\gamma}\right)^2 = \left[H_d + M_s(1 - N_k) + \frac{2A}{\mu_0 M_s}k^2\right] \times \left[H_d + M_s N_k \frac{k_x^2}{k^2} + \frac{2A}{\mu_0 M_s}k^2\right]. \quad (3)$$

Here, $N_k = [1-\exp(-kd)]/kd$ is a k-dependent demagnetization factor for a film of thickness $d$[20], $A$ is the exchange stiffness parameter, $A = 13$ pJ/m. If we naively chose discrete wavevectors $k$ such that $k_x = n_x\pi/L_x$ and $k_y = n_y\pi/L_y$ for integer $n_x$ and $n_y$, the frequencies given by (3) are plotted along the bottom of fig. 1.

The agreement between the eigenfrequencies determined from the dispersion relation and the eigenfrequencies determined from the full micromagnetic calculation is qualitative at best. The discrete values of $\mathbf{k}$ correspond more closely to rectangular samples than to the elliptical shape. For the results shown, we have used the average static demagnetization field $H_d$ is $-N_y M$ = -14.6 kA/m, but there is some ambiguity in this choice. The static micromagnetic calculation yields a field of only $H_d = -6.22$ kA/m at the center of the ellipse where the precession is strongest for many of the modes, but when this value is used, agreement with the dynamic micromagnetic results is worse. A final shortcoming of the simple models is that they do not predict modes corresponding to the end modes.

## III. NANODOT

We have used the spectral mapping technique to look at the eigenmodes of a normally magnetized disk of cobalt, 50 nm in diameter and 16 nm thick with an applied field ranging from 2 T to 4 T along the z direction normal to the circular faces of the disk. Experiments[14] show that the magnetization of this nanodot becomes unstable when the current passing through it exceeds a field-dependent critical current.

The micromagnetic modeling was done with 1 nm cubic cells. Because the thickness of the disk is comparable to the diameter, this is a 3D calculation. Precession was excited by applying a field pulse $H_p(\mathbf{r}) \propto xyz$ only in the region $x > 0$, $y > 0$ and $z > 0$. Modes even

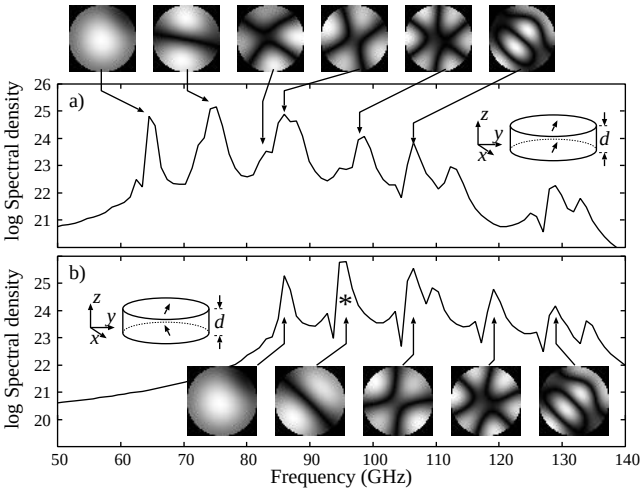


FIG. 2: Normal modes and spectral density for a 16 nm thick, 50 nm diameter cobalt disk for a) modes with even z-symmetry and b) modes with odd z-symmetry. Because the second odd mode is nonuniform both in plane and normal it is most likely to be driven unstable by a spin current.

and odd in $z$ were determined by computing power spectra of $M_x^+(\mathbf{r},t) = M_x(x,y,d,t) + M_x(x,y,0,t)$ for even modes and $M_x^-(\mathbf{r},t) = M_x(x,y,d,t) - M_x(x,y,0,t)$ for odd modes. The power spectra and mode images are shown in fig. 2.

Calculations[17,18] show that the stability or instability of particular modes of the magnetization depend on the competition between the current induced torque and the damping. The current induced torque increases linearly with the current and depends on the geometry of the mode becoming unstable. For the current induced torque to drive a mode of the magnetization in a single layer toward instability, two things are required. First, the mode must be laterally non-uniform so that spins diffusing in the leads from one part of the magnetic layer to another exert a torque. Second, the two interfaces need to be asymmetric, otherwise the torques on both interfaces cancel. This asymmetry can arise in two ways: the leads on the two sides can be asymmetric[17] or the mode that becomes unstable can be non-uniform through the thickness of the layer[18].

The damping, on the other hand, is independent of the current and is proportional to the frequency of the mode being excited when the precession is circular. When the precession is elliptical, the dependence of the damping on the frequency is more complicated. Generally speaking, mode frequencies increase with external magnetic field. This increase leads to an increase in the damping for the mode that becomes unstable, so that the critical current for

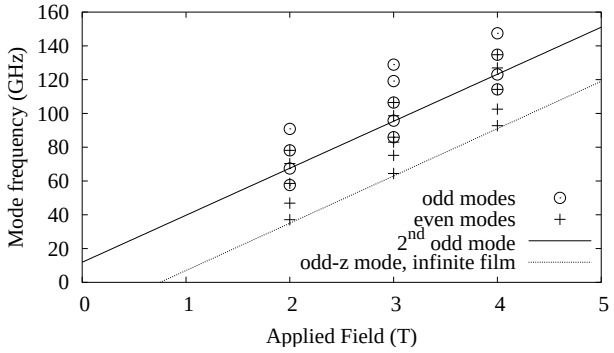


FIG. 3: Applied field dependence of normal mode frequencies. Crosses are for even z-symmetry modes and circles are for odd z-symmetry modes. The upper line shows the extrapolation of the 2nd odd mode to zero field and the lower line shows the mode model used in ref.(CITE)

an instability increases with external field.

Calculations based on the dynamics of a thin film[18]show that the lowest threshold for instability is for a mode odd in z and with a wavelength comparable to the dot diameter. We identify this mode as the second odd mode shown in fig. 2b). Even though other modes have lower frequency and less damping, the greater current induced torque due to the asymmetry in the $n_z = 1$ mode overcomes the extra damping.

One of the prominent features of the experimental data is that the critical current extrapolates to zero as a function of the magnetic field applied normal to the disk[14]. To investigate this behavior, we compute the field dependence of the frequencies of the modes most likely to become unstable. See fig. 3. In agreement with experiment, we find that they extrapolate to zero frequency at a field closer to zero than would be naively expected for thin-film-mode considerations, $\omega = \gamma\mu_0[H - M_s + D(\pi/d)^2]$. However, this agreement is coincidental rather than fundamental and may not be the explanation for the experimental results.

In summary, we have used dynamic micromagnetic techniques to determine the lowest frequency eigenmodes for a magnetic ellipse in zero field and a for a perpendicularly magnetized disk. The eigenfrequencies are only in qualitative agreement with simple models, which fail to predict localized modes at the end of the ellipse. The field dependence of the eigenmode frequencies in the disk mimics the field dependence of the critical currents in a

spin transfer torque experiment.

---


[1] M. Belov, Z. Liu, R. D. Sydora, , and M. R. Freeman, Phys. Rev. B **69**, 094414 (2004).

[2] S. Tamaru, J. A. Bain, R. J. M. Van de Veerdonk, T. M. Crawford, and M. H. Kryder, J. Appl. Phys. **91**, 8034 (2002).

[3] J. P. Park, P. Eames, D. M. Engebretson, J. Berezovsky, and P. A. Crowell, Phys. Rev. B **67**, 020403 (2003).

[4] H. Stoll, A. Puzic, B. van Waeyenberge, P. Fischer, J. Raabe, M. Buess, T. Haug, R. Höllinger, C. Back, and G. Denbeaux, Appl. Phys. Lett. **84**, 3328 (2004).

[5] Y. Acremann, C. H. Back, M. Buess, O. Portmann, A. Vaterlaus, D. Pescia, and H. Melchior, Science **290**, 492 (2000).

[6] Y. Acremann, A. Kashuba, M.Buess, D. Pescia, and C. Back, J. Magn. Magn. Mater. **239**, 346 (2002).

[7] M. Buess, R. Höllinger, T. Haug, U. Krey, D. Pescia, M. R. Scheinfein, D. Weiss, and C. H. Back, Phys. Rev. Lett. **93**, 077207 (2004).

[8] C. Bayer, S. O. Demokritov, B. Hillebrands, and A. N. Slavin, Appl. Phys. Lett. **82**, 607 (2003).

[9] C. Bayer, J. P. Park, H. Wang, M. Yan, C. E. Campbell, and P. A. Crowell, Phys. Rev. B **69**, 134401 (2004).

[10] J. P. Park, P. Eames, D. Engebretson, J. Berezovsky, and P. A. Crowell, Phys. Rev. Lett. **89**, 277201 (2002).

[11] K. Y. Guslienko, S. O. Demokritov, B. Hillebrands, and A. N. Slavin, Phys. Rev. B **66**, 132402 (2002).

[12] K. Y. Guslienko, R. W. Chantrell, and A. N. Slavin, Phys. Rev. B **68**, 024422 (2003).

[13] M. Grimsditch, G. K. Leaf, H. G. Kaper, D. A. Karpeev, and R. E. Camley, Phys. Rev. B **69**, 174428 (2004).

[14] B. Oezyilmaz, A. D. Kent, J. Z. Sun, M. J. Rooks, and R. H. Koch, cond-mat/0403367 (2004).

[15] Y. Ji, C. L. Chien, and M. D. Stiles, Phys. Rev. Lett. **90**, 106601 (2003).

[16] T. Y. Chen, Y. Ji, C. L. Chien, and M. D. Stiles, Phys. Rev. Lett. **93**, 026601 (2004).

[17] M. L. Polianski and P. W. Brouwer, Phys. Rev. Lett. **92**, 026602 (2004).

[18] M. D. Stiles, J. Q. Xiao, and A. Zangwill, Phys. Rev. B **69**, 054408 (2004).

[19] M. J. Donahue and D. G. Porter, OOMMF User's Guide, Version 1.0, Interagency Report NISTIR 6376, National Institute of Standards and Technology, Gaithersburg, MD (Sept 1999).

[20] K. J. Harte, J. Appl. Phys. **39**, 1503 (1968).